Available online at www.pelagiaresearchlibrary.com

Pelagia Research Library

Advances in Applied Science Research, 2015, 6(4):89-94

ISSN: 0976-8610
CODEN (USA): AASRFC

Electron density calculation and structural analysis of $Li_{0.5}Bi_{0.5}TiO_3$ ceramic

M. Nayak and Manas R. Panigrahi*

Electroceramics Lab, Department of Physics, School of Applied Sciences, KIIT University, Bhubaneswar

---

ABSTRACT

$Li_{0.5}Bi_{0.5}TiO_3$ ceramic powder was synthesized by high energy ball milling. The X-ray diffraction pattern of the sample was analyzed in a quantitative manner using rietveld analysis. X-rays is the finger print of a material and the diffracted intensity can be used to dig out a lot of information related to the material. Again to tailored a material it is necessary to understand the geometry of a material in a quantifying manner. So, in this study it is tried to present a indepth study of the material in term of its atomic positions, bond lengths, bond angles and energy density of different levels. Lastly, a simulated structure is presented using all the initial data available and its energy density.

Keywords: X-ray diffraction; Electron density; Rietveld refinement

---

INTRODUCTION

Lead oxide based ferroelectrics, represented by lead zirconate titanate Pb(Zr, Ti)O_3, (PZT) are widely used for piezoelectric actuators, sensors and transducers due to their excellent piezoelectric properties [1-2]. However, lead is a heavy metal and its toxicity is well known. Therefore, it is necessary to develop lead-free piezoelectric ceramics to replace PZT based ceramics. Sodium bismuth titanate ($Na_{0.5}Bi_{0.5}TiO_3$,NBT), discovered by Smolenskii et al. in 1960 [3], is considered to be one of the candidates of lead-free piezoelectric ceramics. However, NBT has a drawback of high conductivity and high coercive field which cause problems in polarizing process [4]. Thus in the same light $Li_{0.5}Bi_{0.5}TiO_3$ ceramic is synthesized using high energy mechanosynthesis. Though this material have been reported some time as a single or in composite form for different applications, its detailed structure is not reported with clarity. In this paper it is tried to present a thorough and detailed structural analysis of the material from x-ray diffraction. A geometrical structure along with its energy density for different levels is also presented.

MATERIALS AND METHODS

In the present study commercial ceramic powders of Bi_2O_3(99 wt%), TiO_2 (99 wt%), and Li_2CO_3 (97 wt%) were used as the raw materials. A powder mixture of these raw materials according to the stoichiometric ratio of $Bi_{0.5}Li_{0.5}TiO_3$ was prepared. The prepared reactant was ball milled for 3 hours in a zirconia vial using 40 zirconia balls at a speed of 300 rpm in an ethanol medium. After ball milling, the obtained slurry was dried at 80℃ for 6 h to remove the ethanol. The products were then grounded in an agate mortar for 1/2 hour. The processed ceramic powder were then structurally characterized by a PANalytical X'pert-MPD X-ray diffractometer (XRD). The XRD data were recorded using Ni-filtered Cu K_α radiation from a highly-stabilized and automated Philips X-ray generator (PW 1830) operated at 30 kV and 20 mA. The generator is coupled with a Philips X-ray powder diffractometer consisting of a PW 3040 mpd controller, PW 1050/51 goniometer of radius 240 mm, and a proportional counter with 1° divergence slit, and 1 mm receiving slit. The step-scan data of step size 0.017° and step scan 0.6 s were recorded for the entire angular range 10–90° .

Theory:

Microstructure characterization of the ball-milled powder samples has been made by employing the Rietveld's whole-profile fitting method based on structure and microstructure refinement [5-6]. The experimental profiles were fitted with the most suitable pseudo-Voigt analytical function because it takes individual care for both the particle size and strain broadening of the experimental profiles. For both the $K_{\alpha 1}$ and $K_{\alpha 2}$ profiles, the line broadening function B (2θ) and the symmetric part of instrumental function S (2θ) may be represented by the pseudo-Voigt function

$$pV(x) = \sum I_{nt}[\eta C(x) + (1-\eta)G(x)] \quad (1)$$

where the Cauchyian component, $C(x) = (1 + x^2)^{-1}$ and the Gaussian component, $G(x) = \exp[-(\ln 2)x^2]$. The powder diffraction patterns were simulated providing all necessary structural information and some starting values of microstructural parameters of the individual phases with the help of the Rietveld software, Fullprof [7-8].

Initially, the positions of the peaks were corrected by successive refinements of zero-shift error. Considering the integrated intensity of the peaks as a function of structural parameters only, the Marquardt least-squares procedures were adopted for minimization of the difference between the observed and simulated powder diffraction patterns and the minimization was carried out by using the reliability index parameter, R_{wp} (weighted residual error), R_{exp} (expected error) and R_B (Bragg factor) defined as:

$$R_{wp} = \left[\frac{\sum w_i (I_0 - I_c)^2}{\sum w_i I_0^2}\right]^{1/2} \quad (2)$$

$$R_B = 100\frac{\sum |I_0 - I_c|}{\sum I_0} \quad (3)$$

and

$$R_{\exp} = \left|\frac{N-P}{\sum w_i I_0^2}\right|^{1/2} \quad (4)$$

where I_0 and Ic are the experimental and calculated intensities, respectively, wi ($1/I_0$) and N are the weight and number of experimental observations, and P is the number of fitting parameters.

The goodness of fit (GoF) is established by comparing R_{wp} with the expected error, $R_{exp.}$. This leads to the value of goodness of fit [9-10]:

$$GOF = \frac{R_{wp}}{R_{\exp}} \quad (5)$$

Refinement continues till convergence is reached

RESULTS AND DISCUSSION

In the present study rietveld profile matching and integrated intensity refinement analysis of X-ray of powder diffraction data is adopted to obtain the refined structural parameters, such as atomic coordinates, occupancies, lattice parameters, microstructural parameters, and energy density using Fullprof version 2.50 Rietveld software. The XRD pattern of LBT ceramic is shown in fig.1. The refinements were conducted without refining the isotropic atomic thermal parameters.

The x-ray pattern shows 3 different major phases, namely, lithium bismuth phosphorous (V) oxide as 68.8%, lithium dioxobismuthate as 29.8% and dilithium tetrabismuth dititanium(III) titanium oxide as 1.4%. matched with with JCPDS data card #(98-001-4563), (98-000-8950) and (98-006-4716) respectively. During refinement process the different structural parameters obtained are enlisted here as, Tip Width,3.79473 Å, Obs. Lorentz B [°2θ]=6.01522, Obs. Gauss B [°2θ]=0.10206, Obs. B [°2θ]=6.04358, Instr. Lorentz B [°2θ]=0.07470, Instr. Gauss B[°2θ] = 0.06328, Instr. B [°2θ]=0.11842, Struct. Lorentz B [°2θ]=5.94052, Struct. Gauss B [°2θ]=0.08008, Struct. B [°2θ]= 5.94160, Universal Shape= 0.52325, Micro Strain [%]= 0.16447, Crystallite Size [Å]= 15.19054. Different structure factor are estimated to be, F observed=170.1585, F calculated=141.3984 and F esd=15.21149 with multiplicity 8.

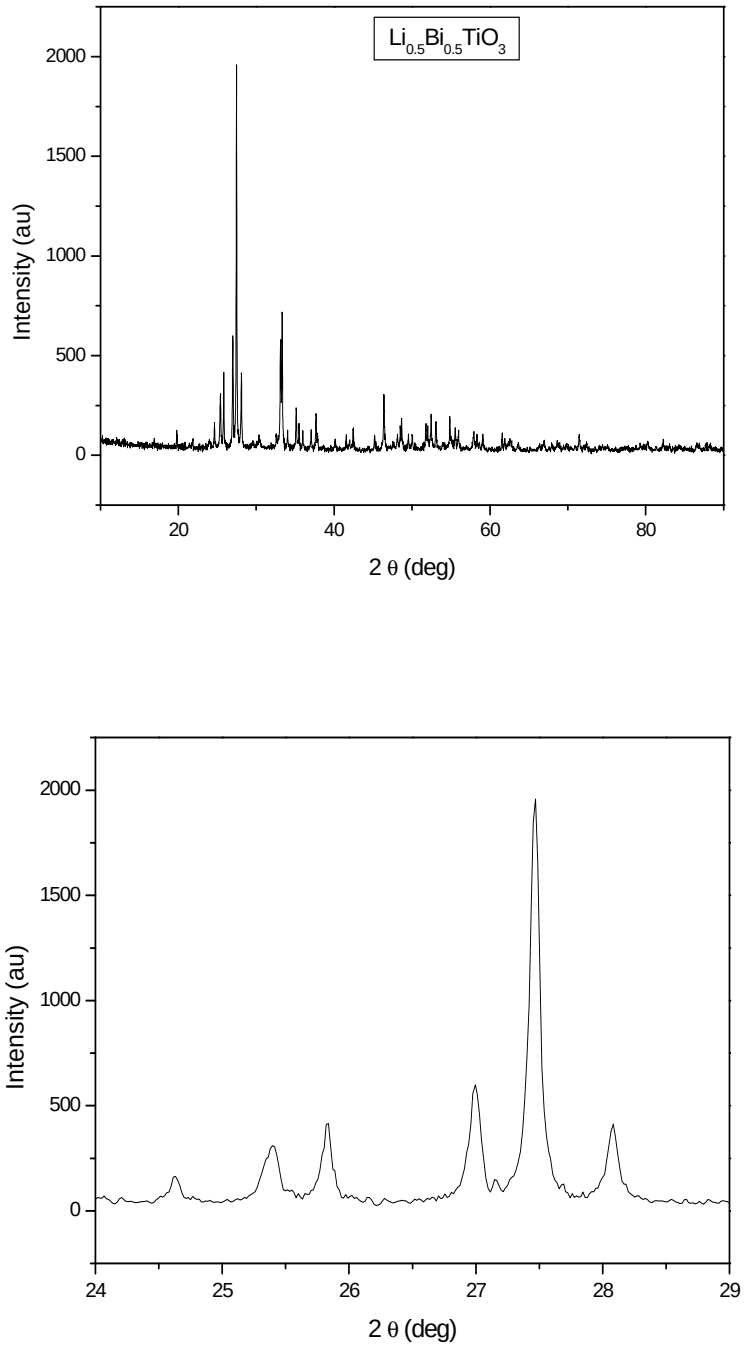

Fig.1 : X-ray Diffraction of $Li_{0.5}Bi_{0.5}TiO_3$ ceramic

Different refined parameters are calculated to be , Rp=37.5410, Rwp=44.7160, Rexp=15.9455 with GOF = 7.8641. The Caglitio width is estimated to be U=10 (2.8066), V=-1(2.3498) and W=2.1634 (0.4496).

After refinement a crystal structure with the following data was obtained. crystal system: orthorhombic, space group=I b a m and space group no.=72. The lattice parameters (Å) are fund to be, a=5.1034 (0.01145), b=17.9131(0.03145) and c=4.8308 (0.0096) with α=β=γ=90˚. Table-1 shows the x-ray diffraction data of $Li_{0.5}Bi_{0.5}TiO_3$ ceramic with inter-planner spacing, crystallite size and (h k l) parameters of individual planes. FWHM and intensity(cts) is also mentioned for the individual planes. The energy density and generated structure from analysis seems to be very interesting with different level of energy. The energy density (ED) from Fourier analysis is given in the **table-2.**

Table-1: X-ray diffraction data of $Li_{0.5}Bi_{0.5}TiO_3$ ceramic

Sl. No.	(2θ)	h k l	d (nm)	FWHM	Cts	D (nm)
1	19.80	1 0 2	0.4481	0.1224	62.97	64.65
2	24.63	1 1 2	0.3611	0.0816	127.05	100.38
3	25.40	2 0 2	0.3504	0.1632	265.45	50.51
4	25.86	2 2 0	0.3442	0.0612	384.63	135.20
5	27.02	2 1 2	0.3297	0.102	1934.35	81.94
6	27.46	3 0 0	0.3246	0.0612	576.35	137.11
7	28.04	1 0 3	0.3180	0.0816	378.99	103.38
8	30.33	3 1 1	0.2945	0.3264	57.83	26.43
9	33.15	3 2 0	0.2701	0.0816	548.74	108.98
10	34.08	3 1 2	0.2628	0.1224	89.08	73.45
11	35.55	0 0 4	0.2523	0.1224	93.76	74.77
12	36.90	4 0 0	0.2434	0.1224	99.98	76.06
13	37.75	3 2 2	0.2381	0.1224	160.01	76.94
14	40.22	2 0 4	0.2403	0.2448	43.30	39.83

Table-2: Energy Density

No.	ED
1	18.719
2	18.631
3	16.831
4	16.438
5	13.505
6	13.505
7	12.015
8	11.979
9	11.597
10	11.597
11	11.565
12	11.501
13	9.999
14	9.908
15	9.889
16	9.889
17	9.717
18	9.564
19	9.080
20	9.080
21	8.861
22	8.666
23	8.665
24	8.665
25	8.665
26	8.156
27	7.848
28	7.848
29	7.650
30	7.650
31	7.423
32	7.398
33	7.398
34	7.140
35	7.139
36	7.102
37	7.102
38	6.997
39	6.997
40	6.992
41	-10.360
42	-10.360
43	-9.863
44	-9.863
45	-8.434
46	-8.145
47	-8.039
48	-7.931

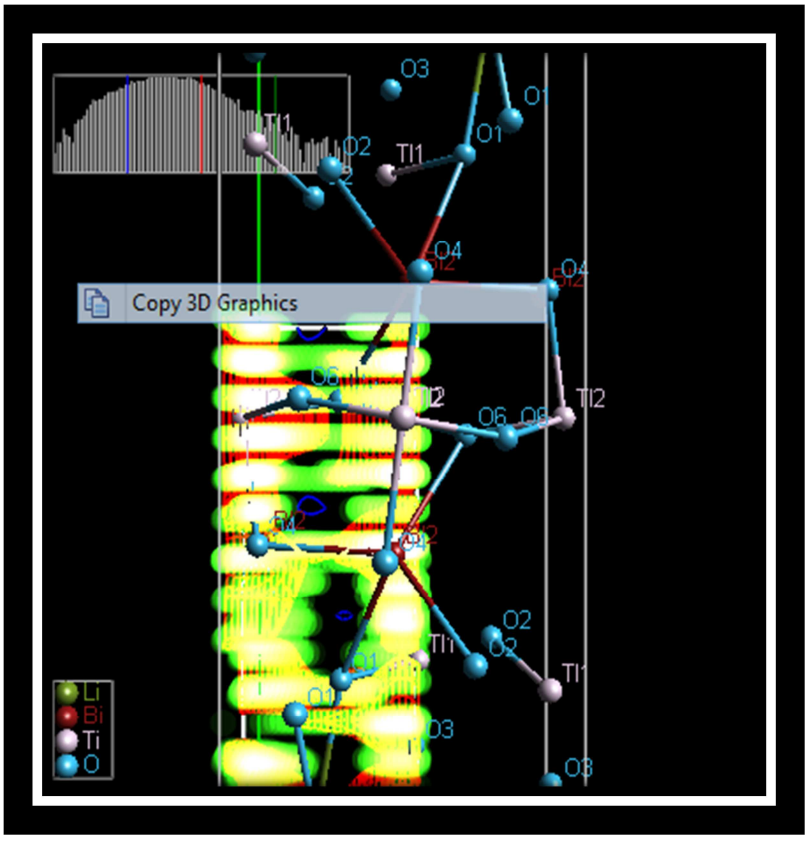

Fig.2 schematic representation of Electron density and structure from Fourier analysis

Table-3: Atomic positions

Sl. No.	Elements	Oxidation state	Wyk.	multiplicity	Sof	B_{iso}	X	Y	Z
1	O	-2	8j	8	1	0.5	0.231	0.412	0
2	O	-2	8j	8	1	0.5	0.239	0.211	0
3	Li	1	8g	8	1	0.5	0	0.25	0.25
4	Bi	3	8j	8	1	0.5	0.2689	0.0893	0

Table-4: Distance and bond angles:

O1	- TI1	2.028	1x
	- LI1	2.210	1x
	- TI1	2.293	1x
	- O3	2.557	1x
	- BI2	2.600	1x
	- O4	2.757	1x
	- O1	2.774	2x
	- O2	2.776	1x
	- O3	2.856	1x
	- O2	2.911	1x
	- BI1	2.994	1x
	- O2	3.163	1x
	- BI2	3.198	1x
	- O4	3.260	1x
	- LI1	3.277	1x
O2	- TI1	1.695	1x
	- TI1	2.031	1x
	- BI2	2.374	1x
	- O4	2.462	1x
	- O3	2.704	1x
	- O2	2.748	2x
	- O1	2.776	1x
	- BI2	2.798	1x
	- O1	2.911	1x
	- O3	2.967	1x
	- O4	2.972	1x
	- O1	3.163	1x
O3	- TI1	1.721	1x
	- LI1	1.865	1x
	- LI1	2.488	1x
	- O1	2.557	1x
	- O5	2.569	1x
	- BI1	2.671	1x
	- BI1	2.701	1x
	- O2	2.704	1x
	- O1	2.856	1x
	- O5	2.951	1x
	- O2	2.967	1x
	- BI1	3.116	1x
	- O5	3.124	1x
	- BI1	3.168	1x
	- O5	3.204	1x
	- BI1	3.453	1x
O4	- TI2	2.105	1x
	- BI2	2.306	1x
	- BI2	2.357	1x
	- TI1	2.409	1x
	- O2	2.462	1x
	- O6	2.739	1x
	- O1	2.757	1x
	- O6	2.874	1x
	- O6	2.910	1x
	- O2	2.972	1x
	- O6	3.122	1x
	- BI2	3.129	1x
	- BI2	3.152	1x
	- O1	3.260	1x
	- O4	3.492	2x
O5	- LI1	1.806	1x
	- BI1	2.118	1x
	- BI1	2.241	1x
	- BI1	2.253	1x
	- BI1	2.478	1x
	- O3	2.569	1x
	- O5	2.729	4x
	- LI1	2.908	1x
	- O3	2.951	1x
	- O3	3.124	1x
	- LI1	3.153	1x
	- O3	3.204	1x
	- LI1	3.344	2x
O6	- TI2	1.890	1x
	- TI2	2.109	1x
	- O6	2.296	1x
	- BI2	2.607	1x
	- O4	2.739	1x
	- O6	2.759	2x
	- O4	2.874	1x
	- O4	2.910	1x
	- BI2	2.942	1x
	- BI2	2.953	1x
	- O4	3.122	1x
	- BI2	3.208	1x
	- O6	3.275	1x
TI1	- O2	1.695	1x
	- O3	1.721	1x
	- O1	2.028	1x
	- O2	2.031	1x
	- O1	2.293	1x
	- O4	2.409	1x
	- LI1	3.083	1x
	- LI1	3.094	1x
	- BI2	3.313	1x
	- BI2	3.365	1x
	- TI1	3.451	2x
TI2	- O6	1.890	2x
	- O4	2.105	2x
	- O6	2.109	2x
	- BI2	3.220	2x
	- BI2	3.395	2x
BI1	- LI1	1.979	1x
	- LI1	2.047	1x
	- O5	2.118	1x
	- O5	2.241	1x
	- O5	2.253	1x
	- O5	2.478	1x
	- O3	2.671	1x
	- O3	2.701	1x
	- O1	2.994	1x
	- O3	3.116	1x
	- O3	3.168	1x
	- LI1	3.330	1x
	- O3	3.453	1x
BI2	- O4	2.306	1x
	- O4	2.357	1x
	- O2	2.374	1x
	- O1	2.600	1x
	- O6	2.607	1x
	- O2	2.798	1x
	- O6	2.942	1x
	- O6	2.953	1x
	- O4	3.129	1x
	- O4	3.152	1x
	- O1	3.198	1x
	- O6	3.208	1x
	- TI2	3.220	1x
	- TI1	3.313	1x
	- TI1	3.365	1x
	- TI2	3.395	1x
LI1	- O5	1.806	1x
	- O3	1.865	1x
	- BI1	1.979	1x
	- BI1	2.047	1x
	- O1	2.210	1x
	- O3	2.488	1x
	- LI1	2.721	2x
	- O5	2.908	1x
	- TI1	3.083	1x
	- TI1	3.094	1x
	- O5	3.153	1x
	- O1	3.277	1x
	- BI1	3.330	1x
	- O5	3.344	2x

Table-3 gives the different atomic positions along with its oxidation states and multiplicity. Multiplicity is found to be 8 even from the Fourier analysis, which support in calculating the energy density. Table-4 represents the bond angles and bond lengths of different atoms of the material. Using the initial information obtained from the quantitative analysis of the material and using the same with the powder cell a clear structure is proposed for the LBT ceramic along with this the different generated atomic positions and other structural parameters with all

possible bond angles and bond lengths between the different Li, Bi, Ti and O- atoms. This gives a clear picture of the material with proper understanding for tailoring the material.

CONCLUSION

A comprehensive structural analysis is done on the basis of X-ray diffraction of the LBT ceramics in terms of its bond lengths, bond angles and the atomic positions of the different atoms. A simulated probable structure is also presented in the study. Above all the energy density of all the atoms at different levels are also presented. By understanding the crystal structure of a material it is always wise to tailored the material as per requirement of technology and situation. This study really gives an insight to the structure of the material.

REFERENCES

[1] Jaffe B, Cook WR, Jaffe H, Piezoelectric Ceramics, Academic, New York, **1971**.
[2] Levassort F, Tran-Huu-Hue P, Ringaard E, Lethiecq M, *J. Eur. Ceram. Soc*., **2001,** 21, 1361.
[3] Smolenskii GA, Isupv VA, Afranovskaya AI, Krainik NN, *J. Sov.Phys. Sol. Stat.*, **1961,** 2, 2651.
[4] He T, Dai J, Tian J, et al., *Ceramics International*, **2008,** 34, 1561.
[5] Rietveld HM, *Acta Crystallogr*. , **1967,** 22, 151.
[6] Warren BE, X-ray Diffraction, Addition-Wesley, Reading, MA, **1969,** p. 264.
[7] Panigrahi MR, Panigrahi S, *Physica B: Condensed Matter*, **2010,** 405, 2844.
[8] Rietveld HM, *J. Appl. Crystallogr*. , **1969,** 265.
[9] Young RA, (Ed.), The Rietveld Method, Oxford University Press/IUCr, **1969,** 1–38.
[10] Panigrahi MR, Panigrahi S, *International Journal of Material Science*, **2010,** 5, 651.